Ultramicroscopy 108 (2008) 1551–1557

Contents lists available at ScienceDirect

Ultramicroscopy

journal homepage: www.elsevier.com/locate/ultramic

Charge drives for scanning probe microscope positioning stages

A.J. Fleming [a,*], K.K. Leang [b]

[a] School of Electrical Engineering and Computer Science, University of Newcastle, Callaghan, NSW 2308, Australia
[b] Department of Mechanical Engineering, University of Nevada, Reno, Reno, NV 89557, USA

ARTICLE INFO

Article history:
Received 2 December 2007
Received in revised form
2 April 2008
Accepted 6 May 2008

PACS:
07.79.−v
07.50.Ek

Keywords:
Tip scanning instrument design and characterization
Scanning tunneling microscopy (STM)
Atomic force microscopy (AFM)

ABSTRACT

Due to hysteresis exhibited by piezoelectric actuators, positioning stages in scanning probe microscopes require sensor-based closed-loop control. Although closed-loop control is effective at eliminating non-linearity at low scan speeds, the bandwidth compared to open loop is severely reduced. In addition, sensor noise significantly degrades achievable resolution in closed loop.

In this work, charge drives are evaluated as a simple positioning alternative when feedback control cannot be applied or provides inadequate performance. These situations arise in high-speed imaging, where position sensor noise can be large or where no feedback sensors are present.

Charge drives can reduce the error caused by hysteresis to less than 1% of the scan range. We review the design of charge drives and compare them to voltage amplifiers for driving lateral SPM scanners. The first experimental images using charge drive are presented.

1. Introduction

A key component of scanning probe microscopes (SPMs) [1] is the nanopositioning system required to maneuver the probe or sample. Piezoelectric actuators are universally employed in positioning systems due to their high stiffness, compact size and effectively infinite resolution. However, a major disadvantage of piezoelectric actuators is the hysteresis exhibited at high electric fields. To avoid imaging artifacts, SPMs require some form of compensation for the positioning non-linearity. Techniques to accomplish this, including feedback, feedforward and image-based compensation are reviewed in Refs. [2–4].

The most popular technique for compensation in commercial SPMs is sensor-based feedback control using integral or proportional–integral (PI) control. Such controllers are simple, robust to modeling error, and due to high loop gain at low frequencies, effectively reduce piezoelectric non-linearity. However, disadvantages of closed-loop control include cost, additional complexity, limited bandwidth and sensor-induced noise.

In this work, the technique of charge control is evaluated for linearization of SPM positioning stages. The aim is to provide a simple alternative to feedback control where such techniques cannot be applied or provide inadequate performance. For example, in high-speed imaging [5–8], it is difficult or impossible to achieve a satisfactory controller bandwidth. Sensor noise is another major issue when atomic resolution is required, particularly if the controller bandwidth is greater than a few Hertz. Also, in many 'homemade' and application specific microscopes, feedback sensors are not present and the only control option is open loop, as is the case in all the scanners reported in Refs. [5–8].

Since the late 80s, it has been known that driving piezoelectric transducers with current or charge rather than voltage significantly reduces hysteresis [9]. Simply by regulating the current or charge, a fivefold reduction in the hysteresis can be achieved [10]. Although the circuit topology of a charge or current amplifier is much the same as a simple voltage amplifier, the uncontrolled nature of the output voltage typically results in the load capacitor being linearly charged. Recent developments have eliminated low-frequency drift and permitted grounded loads, which are necessary in nanopositioning systems [11].

In the following section, charge drives are briefly reviewed, then applied to imaging experiments in Section 3. A critical evaluation of charge drives in open- and closed-loop SPM applications is provided in Sections 4 and 5. Implementation options on multi-electrode tubes are then discussed in Section 6 followed by conclusions in Section 7.

2. Charge drives

Consider the simplified diagram of a grounded-load charge drive shown in Fig. 1 [11]. The piezoelectric load, modeled as a

* Corresponding author. Tel.: +61 2 4921 6493; fax: +61 2 4921 7058.
E-mail address: Andrew.Fleming@newcastle.edu.au (A.J. Fleming).

0304-3991/$ - see front matter © 2008 Elsevier B.V. All rights reserved.
doi:10.1016/j.ultramic.2008.05.004

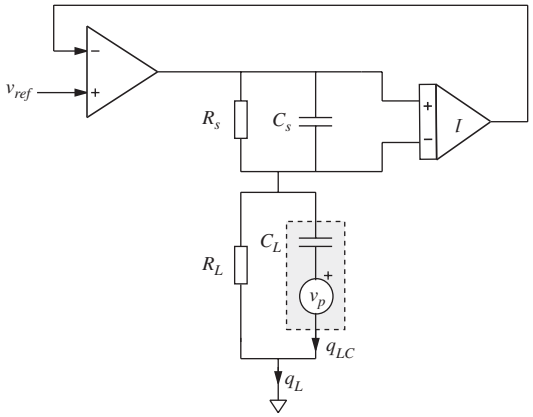

Fig. 1. DC accurate charge drive for grounded capacitive loads [7].

capacitor and voltage source v_p, is shown in gray. The high-gain feedback loop works to equate the applied reference voltage v_{ref}, to the voltage across a sensing capacitor C_s. Neglecting the resistances R_L and R_s, at frequencies well within the bandwidth of the control loop, the load charge q_L is equal to

$$q_L = v_{ref} C_s, \tag{1}$$

i.e., the gain is C_s C/V. When connected to a capacitive load, the equivalent voltage gain is C_s/C_L.

As discussed in Ref. [11], the existence of R_L and R_s introduces error at low frequency. By setting the ratio of resistances equal to the ratio of capacitances, low-frequency error can be eliminated. That is, by setting

$$\frac{R_L}{R_s} = \frac{C_s}{C_L} \tag{2}$$

the amplifier has a constant gain C_s C/V over all frequencies.

Although the parallel resistances act to stabilize the voltage gain at low frequencies, the amplifier now operates as a voltage source below $1/2\pi R_L C_L$ Hz and a charge drive above [11]. A consequence is that reduction of hysteresis only occurs at frequencies above $1/2\pi R_L C_L$ Hz. This cut-off frequency can be reduced by increasing R_L, however, a practical limit is imposed by the dielectric leakage of the transducer. Excessively high resistances also reduce immunity to drift resulting from current leakage to or from the high-impedance node between the two capacitors.

The high frequency bandwidth of a charge drive is limited by the same factors as a voltage amplifier. Bandwidth is limited by a secondary pole in the feedback loop formed by the output impedance and load capacitance. Due to additional phase lag contributed by this secondary pole, the amplifiers bandwidth is restricted to around one-tenth the pole's frequency if large stability margins are to be retained.

In addition to the secondary pole discussed above, charge drives are also limited by the bandwidth of the differential amplifier in the charge measuring circuit. If this is near or less than the frequency of the secondary pole, it will degrade phase margin and necessitate a reduction in bandwidth. Although high voltage differential amplifiers such as the AD629 are available for a few dollars, discrete designs can achieve much higher bandwidths, but with increased complexity. If closed-loop bandwidths of greater than a few kHz are required, a high-performance differential amplifier is mandatory.

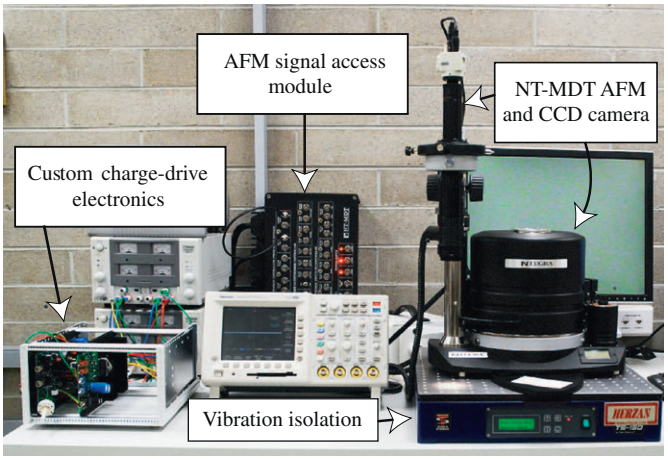

Fig. 2. A photograph of the experimental SPM system with charge drive electronics.

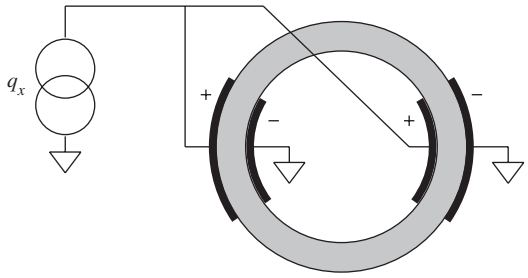

Fig. 3. Top view of the tube scanner. The x-axis electrodes are quartered on the inside and outside and driven in parallel by the charge source.

3. Experimental imaging

Pictured in Fig. 2, an NT-MDT Ntegra SPM was retrofitted with a charge drive on the fast scanning x-axis. A signal access module allowed direct access to the scanner electrodes and reference signal. The charge gain was set to provide an equivalent voltage gain equal to the standard internal controller gain of 15. Accordingly, no modifications to the scan controller or software interface were required.

The scanner is an NT-MDT Z50309cl piezoelectric tube scanner with 100 μm range. As shown in Fig. 3, the tube has quartered internal and external electrodes that allow the scanner to be driven in a bridged configuration. That is, where the internal and external electrodes are driven with equal but opposite voltages. The naming arises from the way in which the electrodes 'bridge' the two driving sources together, effectively doubling the differential voltage experienced by the actuator. Compared to the more popular grounded internal electrode configuration, the bridged configuration requires half the driving voltage to achieve full range. In these experiments one pair of electrodes were grounded to allow an analogy with stack-based positioners that are driven with this configuration. Further discussion specific to piezoelectric tube scanners, including the application of charge drives to bridged electrodes, is contained in Section 6.

During imaging, the atomic force microscope (AFM) was operated in constant height, contact mode, using a cantilever with spring constant 0.2 N/m. The lateral deflection of the piezo actuator was measured using capacitive sensors incorporated into

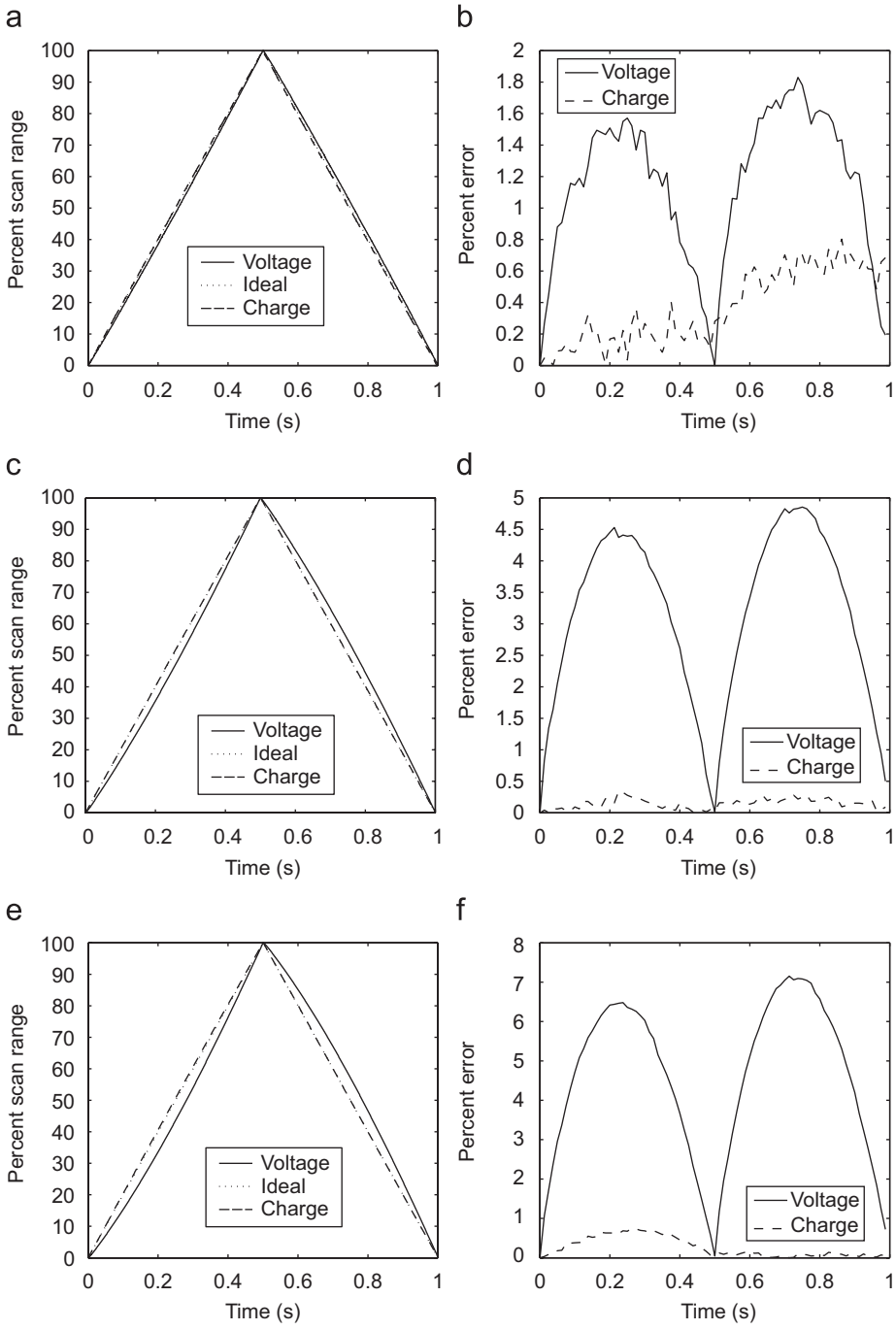

Fig. 4. The measured scanner deflection and percentage error for 5, 20 and 50 μm scans. The input was a 1 Hz triangle wave.

the scanner assembly. A 1-Hz triangle wave was applied to develop scans of 5, 20 and 50 μm, corresponding to 5%, 20% and 50% of the maximum scan range. The scanner trajectories and tracking errors are plotted in Fig. 4. Maximum absolute error for voltage and charge drive is compared in Table 1.

The displacement non-linearity was only 2% in the 5-μm voltage-driven scan; this was reduced to 0.86% using charge actuation. In the 20 and 50-μm scans, voltage-driven non-linearity was more significant, 4.9% and 7.2%, respectively. This was reduced to 0.36% and 0.78% using charge, a reduction of 93% and 89%.

AFM images of a 20-nm feature-height parallel calibration grating (3-μm pitch) are pictured in Fig. 5. Images were recorded by linearizing the *y*-axis with a capacitive sensor and driving the *x*-axis with voltage, then charge. For the 5-μm scan in Fig. 5(a), the 2% voltage non-linearity is not discernable. However, for the 20 and 50-μm scans in Fig. 5(c) and (e), the 4.9% and 7.2% non-linearity clearly distorts the image. In all three charge-driven

Table 1
Open-loop scan error with voltage and charge actuation

Scan range (μm)	Absolute scan error		Reduction (%)
	Voltage (%)	Charge (%)	
5	2.0	0.86	54
20	4.9	0.36	93
50	7.2	0.78	89

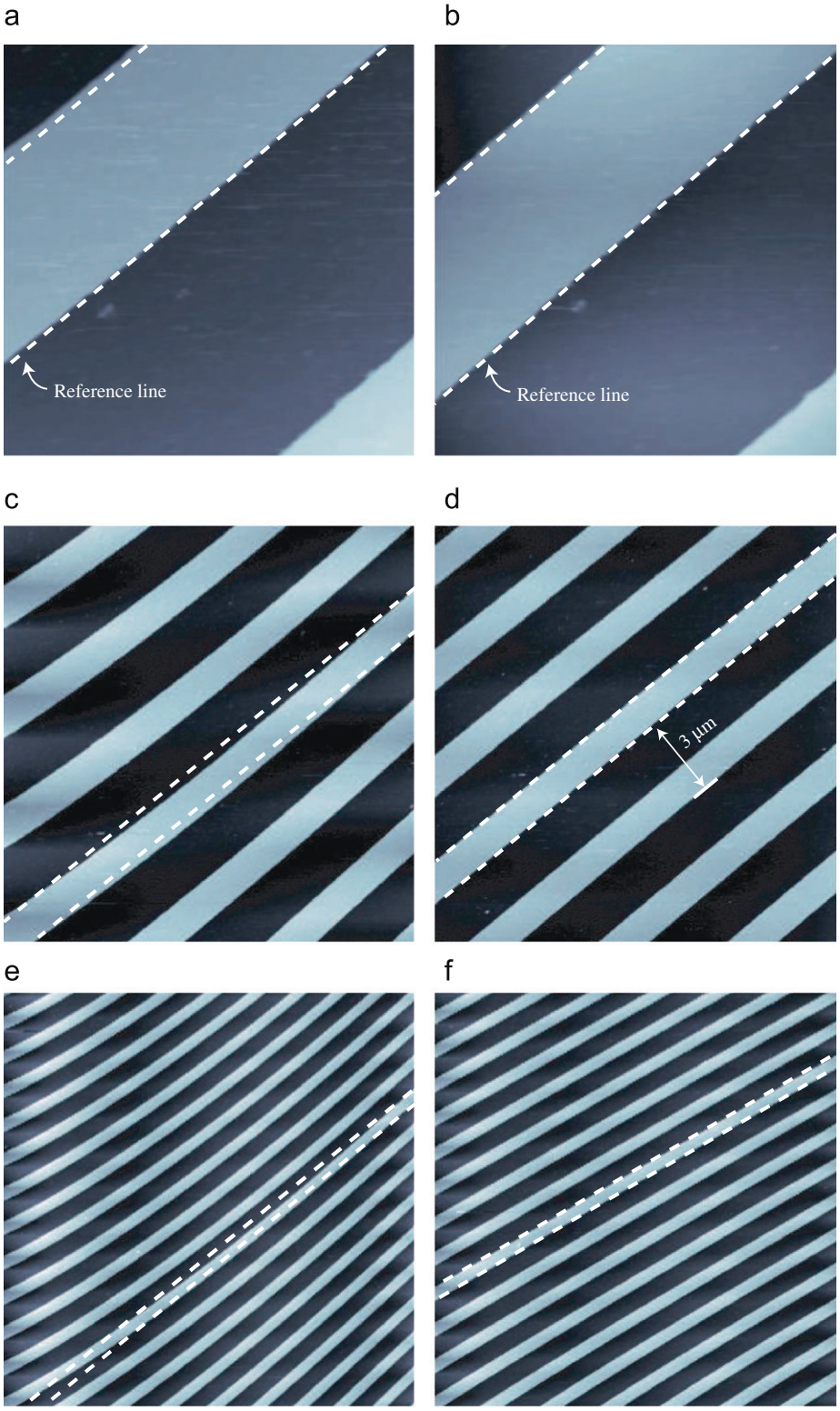

Fig. 5. A comparison of images recorded using voltage and charge actuation. The sample is a periodic calibration grating with 20 nm feature height.

scans, Fig. 5(b), (d) and (f), the non-linearity is less than 1% and image distortion is imperceptible. Reference lines in Fig. 5 are superimposed on each image for comparison.

4. Charge versus voltage

In this section, advantages and drawbacks of charge drives are discussed for open-loop positioning applications.

4.1. Advantages

There are two motivating factors for the use of charge drives in SPM's reduction of hysteresis and vibration compensation.

In Section 3, the non-linearity of a tube scanner driven to half its full-scale range was measured at 7.2%. Subsequent images demonstrate that this magnitude of error is intolerable. Conversely, when driven with charge, scan error remains below 1%

and is imperceptible in images. Thus, while closed-loop control of voltage-driven AFM scanners is mandatory, the use of charge drives can provide satisfactory linearity with no feedback. Follow-on benefits include zero sensor-induced noise, no controller imposed bandwidth limitations, simpler scanner design (due to the absence of sensors) and lower cost.

In high-speed AFM systems [5–8] where feedback control is not feasible, the use of charge drives has the potential to significantly increase imaging performance. Feedback control is not an option due to bandwidth and noise considerations.

In addition to hysteresis reduction, damping of resonant modes can also be accomplished without the need for feedback. In Ref. [11], shunt damping of scanner modes was accomplished by implementing a passive impedance in parallel with the scanner electrodes. The impedance is tuned to resonate with the transducers capacitance at the frequency of problematic modes. Greater than 20 dB attenuation of the first lateral mode was demonstrated [11].

With hysteresis significantly reduced by charge drive, linear feedforward approaches [4] can also be implemented with high accuracy.

4.2. Disadvantages

The disadvantages of charge drives are the increased circuit complexity, voltage range reduction and necessity for gain tuning.

Although floating-load charge drives are similar to standard inverting voltage amplifiers, the grounded-load configuration in Fig. 1 requires a high-performance differential buffer. The differential buffer requires high-input impedance, common-mode range equal to the high-voltage supply and common-mode-rejection ratio greater than 80 dB over the bandwidth of the amplifier. These specifications are not met by available integrated devices but can be achieved with discrete designs, with increased circuit complexity. However, if the application does not require operation beyond 100 Hz, the differential buffer can be constructed easily with off-the-shelf parts, for example the AD629.

The differential buffer present in the grounded-load configuration contributes some additional noise which is likely to be greater than the thermal noise of resistors in a voltage feedback amplifier. Thus, a grounded-load charge drive will generate more noise than a voltage amplifier of the same gain. The situation is different for a floating-load charge drive. This does not require a differential buffer and can provide less noise than a comparable voltage amplifier as the feedback network does not contribute thermal noise.

In addition to amplifier noise, electromagnetic interference can contribute strongly to circuits with high-impedance nodes. In this regard, the grounded-load configuration is superior to the floating-load configuration as it is more easily shielded.

Due to the voltage drop across the sensing capacitor C_s, the output voltage range is limited by the maximum amplifier voltage minus the feedback voltage. This requires a slightly higher supply voltage to develop the same transducer displacement. For high-voltage devices greater than 100 V, the maximum 10 V drop across C_s is not significant. However, in lower voltage applications, this reduction may become significant as standard ICs are limited to between 36 and 50 V. Simply increasing C_s and decreasing V_{ref} is an option for improving voltage range.

Aside from issues with the actual circuitry, the only significant difference between voltage and charge actuation is the need to adjust charge gain. At DC and low frequencies, the voltage gain is fixed by the ratio of resistances R_L and R_s—these are easily interchanged or adjusted. To achieve the same gain at higher frequencies, C_s would need to be adjusted accordingly. This is impossible as variable capacitors of sufficient capacitance are not available. A better option is to select C_s larger than necessary, then add a gain α to the differential buffer, this allows a reduction of charge gain to that desired. After the charge gain is set, the resistance ratio R_L/R_s needs to be adjusted to $\alpha C_s/C_L$.

5. Impact on closed-loop control

At normal imaging speeds, i.e., less than 10 Hz scan rate, simple integral controllers with either damping controllers or notch filters for resonance compensation provide sufficient performance and are widely applied [12]. Over the frequency range where loop gain is greater than 1, typically from DC to tens of Hz, the scanner displacement tracks additive sensor noise. Even with low-noise capacitive sensors (noise density $20\,\mathrm{pm}/\sqrt{\mathrm{Hz}}$), a controller bandwidth of 100 Hz results in greater than 1-nm peak–peak noise. This precludes standard closed-loop scanners from achieving atomic resolution. The situation can be improved by dropping the controller bandwidth to 10 Hz. Although this provides the possibility for atomic resolution, the limited bandwidth restricts usage to extremely slow scanning only.

With charge control of the fast axis, sensors are not required for linearization. Thus, no sensor induced noise is present. However, to eliminate creep and thermal drift in the scanner, a slow feedback loop can be added. In this case, sensor noise is negligible as the bandwidth of such a control loop would be less than 1 Hz.

Charge drives are also suited to systems containing feedforward controllers. Many linear feedforward controllers have been proposed that significantly improve the speed and accuracy of positioning stages with little added complexity, a review of such techniques can be found in Refs. [2–4]. In the past, a major drawback of linear feedforward control has been the inability to reduce hysteresis. When using charge drives, hysteresis is heavily reduced and feedforward control can be effectively applied, even at high scan ranges [13].

6. Alternative electrode configurations

Commercial SPMs that contain piezoelectric tube scanners utilize one of two possible electrode configurations: the grounded internal electrode configuration, or quartered internal electrode configuration. The application of charge drives to each of these scenarios is discussed below.

The techniques discussed in this section are not relevant to piezoelectric stack-based scanners. These actuators are unipolar and require only a single voltage or charge source with one grounded electrode. This configuration is used in the previous sections.

6.1. Grounded internal electrode

The most common electrode configuration on piezoelectric tube scanners is a single grounded internal electrode with quartered external electrodes. Electrodes on opposite sides are driven with equal but opposite voltages to induce deflection in that axis. Unfortunately, although the tubes themselves are simple to fabricate, this configuration requires two bipolar voltage amplifiers for each electrode, four in total to achieve x and y lateral motion.

As charge drives are more complicated than voltage amplifiers it is undesirable to require four of them. However, the drive requirements can be simplified if the two electrodes are mechanically and electrically identical. If so, the voltage induced

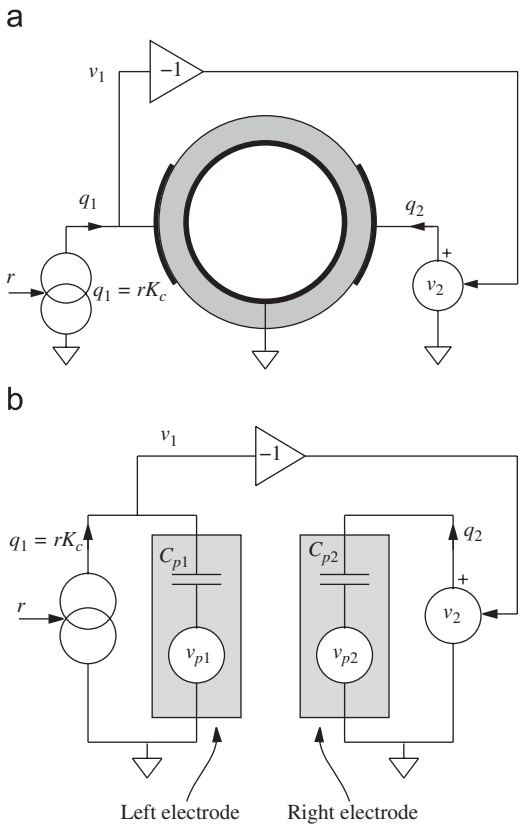

Fig. 6. The grounded internal electrode configuration (top) and equivalent electrical circuit (bottom).

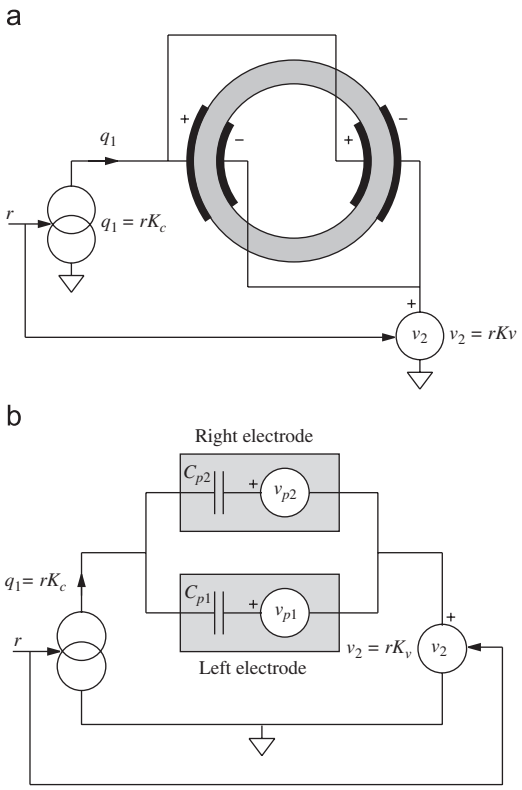

Fig. 7. The quartered, or bridged internal electrode configuration (top) and equivalent electrical circuit (bottom).

on the charge-driven electrode can simply be negated and applied to the opposite electrode as shown in Fig. 6(a). For an explanation, consider the electrical equivalent circuit in Fig. 6(b). The piezoelectric elements under each left- and right-hand electrode are modeled as the capacitances c_{p1} and c_{p2} in series with the piezoelectric strain voltages v_{p1} and v_{p2}. As the electrodes are on opposite sides of the tube, and equal but opposite voltages are applied to both electrodes, the piezoelectric strain voltages v_{p1} and v_{p2} will also be equal but opposite. Under this assumption, if the voltage v_1 is applied oppositely to the right-hand electrode, i.e., if $v_2 = -v_1$, the charge q_2 will be equal but opposite to q_1, and the tube will behave linearly as if two independent charge drives were used.

6.2. Quartered internal electrode

As illustrated in Fig. 3 and discussed in Section 3, the quartered internal electrode configuration, although more difficult to fabricate, requires half the voltage of the previous technique to achieve the same deflection. This is a major advantage as high-voltage amplifiers are costly and two independent amplifiers are required for each axis.

The application of a charge drive to bridged electrodes is somewhat different from the standard voltage-driven configuration. Usually opposite voltages are applied to the inner and outer electrode while the left- and right-hand electrode pairs are connected in parallel. As the bridged electrodes connect the two sources in series, two charge drives would not form a stable circuit. This is analogous to connecting two voltage sources in parallel.

A suitable electrical connection that requires only a single charge drive is shown in Fig. 7. Interestingly, varying the voltage on the electrodes marked negative does not alter the amount of deposited charge or corresponding displacement. However, by setting the voltage on the negative electrode approximately equal but opposite to the voltage developed by the charge drive, twice as much charge can be deposited with the same voltage. So far as the charge drive is concerned, driving the negative electrodes with an opposite voltage results in a doubling of the load capacitance. Thus, twice as much charge can be deposited with the same voltage.

The electrical equivalent circuit of a charge-driven tube with internal electrodes is contained in Fig. 7(b). If a reference signal r is applied to a charge amplifier with gain K_c C/V, the load voltage will be approximately

$$v_1 = rK_c/C_p \tag{3}$$

(neglecting v_{p1} and v_{p2} that are much lesser than $v_1 - v_2$), where C_p is the parallel combination of C_{p1} and C_{p2}. Thus, if the voltage gain K_v is set to $K_v = -K_c/C_p$, the voltage v_2 will be approximately $-v_1$ and the charge drive will result in an approximately balanced voltage across the load. Another option is to adopt a similar approach to the previous section; however, this requires additional circuitry to buffer and measure the voltage developed by the charge drive (v_1).

The configuration in Fig. 7(a) was implemented on the experimental setup discussed in Section 3. The bridged load allowed a 200 V charge drive to obtain the full 400 V differential required for maximum deflection. An experimental 100 μm scan comparing both voltage and charge actuation is plotted in Fig. 8. At full range, the maximum scan error using voltage is 9.7%, compared to 2.0% using charge.

It is interesting to note the asymmetry of non-linearity in Figs. 4 and 8. The decreasing part of the charge-driven scan has less non-linearity in all cases. In fact, the maximum scan error, even at full range with bridged electrodes is only 0.5% compared to 9.7% using voltage.

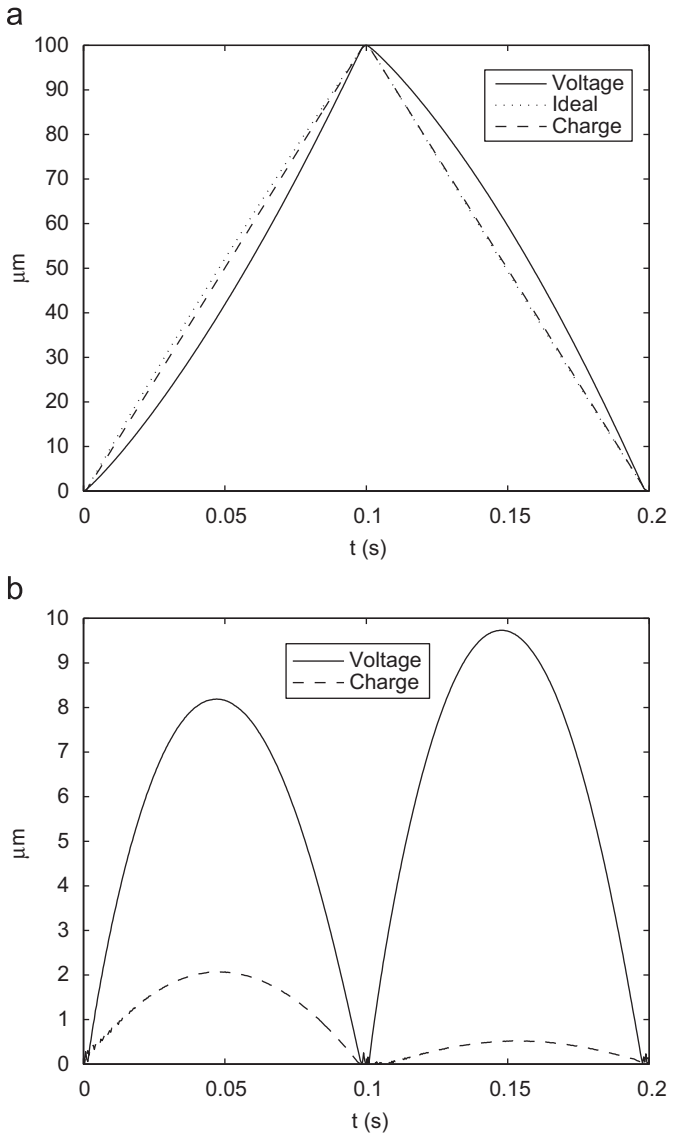

Fig. 8. The bridged voltage and charge-driven deflection in response to a 5 Hz triangle wave (top) and scan error (bottom).

7. Conclusions

In this work, charge drives were evaluated for SPM positioning stages. The advantages are:

- reduction of hysteresis to less than 1% of the scan range,[1]
- straightforward replacement for voltage amplifiers and
- compatible with sensorless vibration control.

Disadvantages include:

- greater circuit complexity,
- requires tuning to set the gain and
- low-frequency performance is limited by the transducer capacitance.

Future work includes developing charge drives for video-speed operation of stack-based positioners.

Acknowledgments

This research was supported by the Australian Research Council (DP0666620) and the Centre for Complex Dynamic Systems and Control. Experiments were conducted at the Laboratory for Dynamics and Control of Nanosystems, University of Newcastle.

References

[1] E. Meyer, H.J. Hug, R. Bennewitz, Scanning Probe Microscopy. The Lab on a Tip, Springer, Heidelberg, Germany, 2004.
[2] Q. Zou, K.K. Leang, E. Sadoun, M.J. Reed, S. Devasia, Asian J. Control 6 (2) (2004) 164.
[3] D.Y. Abramovitch, S.B. Andersson, L.Y. Pao, G. Schitter, A tutorial on the mechanisms, dynamics, and control of atomic force microscopes, in: Proceedings of American Control Conference, New York City, NY, 2007, pp. 3488–3502.
[4] S. Devasia, E. Eleftheriou, S.O.R. Moheimani, IEEE Trans. Control Syst. Technol. 15 (5) (2007) 802.
[5] T. Ando, N. Kodera, T. Uchihashi, A. Miyagi, R. Nakakita, H. Yamashita, K. Matada, J. Surface Sci. Nanotechnol. 3 (2005) 384.
[6] G. Schitter, K.J. Åström, B.E. DeMartini, P.J. Thurner, K.L. Turner, P.K. Hansma, IEEE Trans. Control Syst. Technol. 15 (5) (2007) 906.
[7] A.D.L. Humphris, M.J. Miles, J.K. Hobbs, Appl. Phys. Lett. 86 (2005) 034106-1.
[8] M.J. Rost, L. Crama, P. Schakel, E. van Tol, G.B.E.M. van Velzen-Williams, C.F. Overgauw, H. ter Horst, H. Dekker, B. Okhuijsen, M. Seynen, A. Vijftigschild, P. Han, A.J. Katan, K. Schoots, R. Schumm, W. van Loo, T.H. Oosterkamp, J.W.M. Frenken, Rev. Sci. Instrum. 76 (5) (2005) 053710-1.
[9] C.V. Newcomb, I. Flinn, IEE Electron. Lett. 18 (11) (1982) 442.
[10] P. Ge, M. Jouaneh, IEEE Trans. Control Syst. Technol. 4 (3) (1996) 209.
[11] A.J. Fleming, S.O.R. Moheimani, IEEE Trans. Control Syst. Technol. 14 (1) (2006) 33.
[12] K.K. Leang, S. Devasia, IEEE Trans. Control Syst. Technol. 15 (5) (2007) 927.
[13] G.M. Clayton, S. Tien, S. Devasia, A.J. Fleming, S.O.R. Moheimani, Mechatronics 18 (5–6) (2008) 273.

[1] At full range with quartered internal electrodes, the maximum error due to hysteresis is 2% for the increasing part of the scan and 0.5% for the decreasing part.